Near-field scanning photocurrent microscopy of a nanowire photodetector

Y. Gu
Department of Materials Science and Engineering, Northwestern University, Evanston, Illinois 60208

E.-S. Kwak
Department of Chemistry, Northwestern University, Evanston, Illinois 60208

J. L. Lensch and J. E. Allen
Department of Materials Science and Engineering, Northwestern University, Evanston, Illinois 60208

T. W. Odom
Department of Chemistry, Northwestern University, Evanston, Illinois 60208

L. J. Lauhon[a)]
Department of Materials Science and Engineering, Northwestern University, Evanston, Illinois 60208

(Received 3 March 2005; accepted 10 June 2005; published online 20 July 2005)

A near-field scanning optical microscope was used to image the photocurrent induced by local illumination along the length of a metal-semiconductor-metal (MSM) photodetector made from an individual CdS nanowire. Nanowire MSM photodetectors exhibited photocurrents $\sim 10^5$ larger than the dark current (<2 pA) under uniform monochromatic illumination; under local illumination, the photoresponse was localized to the near-contact regions. Analysis of the spatial variation and bias dependence of the local photocurrent allowed the mechanisms of photocarrier transport and collection to be identified, highlighting the importance of near-field scanning photocurrent microscopy to elucidating the operating principles of nanowire devices. © *2005 American Institute of Physics*. [DOI: 10.1063/1.1996851]

One-dimensional nanomaterials are being considered as the basis of a variety of device technologies. Semiconductor nanowires and carbon nanotubes, for example, have been used to make nanoscale photodetectors with reasonable efficiencies and unique features such as polarization-sensitive detection.[1,2] The mechanisms of carrier photogeneration have been addressed in a number of studies,[2–4] but charge transport and collection in nanowire/nanotube photodetectors have received comparatively little attention[5] and are not well understood. In this regard, photoconductivity measurements employing uniform illumination (spot size larger than the device) may be insufficient to establish the operational principles of nanowire devices because (1) unlike the illumination, the internal electric fields may be highly nonuniform, especially near the metal contacts and (2) similarities between conventional and nanowire device characteristics may be fortuitous. To understand the global response and the ultimate potential of nanowire photodetectors, an understanding of the photoresponse on a smaller length-scale is desirable.

Here we report the application of a near-field scanning optical microscope (NSOM) to map the local photocurrent in individual CdS nanowires configured as metal-semiconductor-metal (MSM) photodetectors. Under local illumination (excitation spot size less than device size), the response of these devices was limited to regions near the M–S contact. Analysis of the spatial variation and bias dependence of the local photocurrent allowed the mechanisms of photocarrier transport and collection to be identified, highlighting the importance of this new local probe technique for elucidating the operating principles of nanowire-based devices.

CdS nanowires (NWs) were synthesized using thermal chemical vapor deposition and gold-catalyzed vapor liquid solid growth;[6] CdS (*n*-type as synthesized) was chosen because of its visible band gap and the extensive literature concerning its bulk photoresponse. Two-terminal NW photodetectors were fabricated using electron beam lithography followed by evaporation of Ti/Au electrodes and liftoff. The device substrates were degenerately doped silicon capped with 400 nm of SiO_2. Optical excitation was provided by a chopped (1 kHz), frequency-doubled Ti:sapphire laser focused by an UV microscope objective, and photocurrent was measured using a current preamplifier and lock-in detection. The NW photodetector was $\sim 10^5$ times more conductive under uniform illumination ($\lambda = 400$ nm, 0.7 W/cm^2) than in the dark [Fig. 1(a)]. The room temperature dark current was less than 2 pA at moderate biases, and the curve shape [Fig. 1(a) inset] is consistent with the formation of back-to-back M–S diodes[7] due to the Schottky barrier between Ti and CdS.[8] The metal electrodes are optically opaque, and no photoresponse was observed under 800 nm excitation; these observations indicate that the photocurrent results from the generation of free carriers within the CdS-NW. The response time of the photodetector circuit was found to be less than 15 μs (the transient response limit of our current preamplifier), which is relatively fast compared to recently reported GaN[4] and ZnO[9] NW photodetectors.

Under global illumination, the NW $I_{ph}-V$ appears very similar to that of a planar MSM photodetector,[7] including the saturation behavior observed at high biases. In the present case, however, the operating principles are not the same, as revealed by local photoexcitation measurements. Figure 1(b) shows two $I_{ph}-V$ curves taken with an NSOM tip (diameter

a)Author to whom correspondence should be addressed; electronic mail: lauhon@northwestern.edu

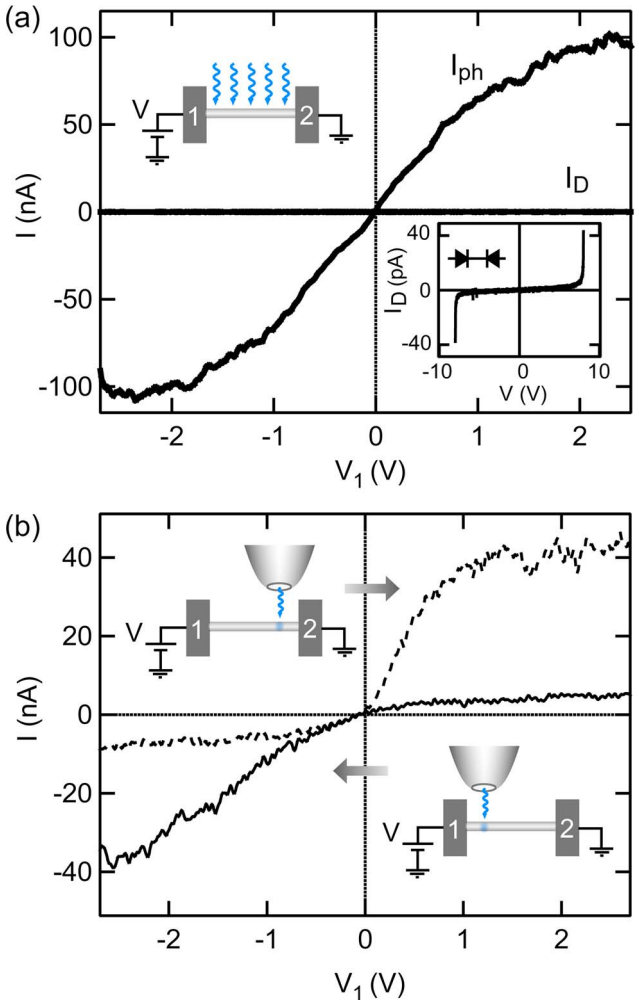

FIG. 1. (a) $I-V$ under uniform 400 nm illumination (I_{ph}) and in the dark (I_D). Inset (upper-left): Device schematic for uniform illumination. Inset (lower-right): dark $I-V$ with a diagram of a generic MSM photodiode; (b) $I-V$ under local illumination near electrode 1 (solid line) and electrode 2 (dashed line). Insets: diagram of NSOM tip positions.

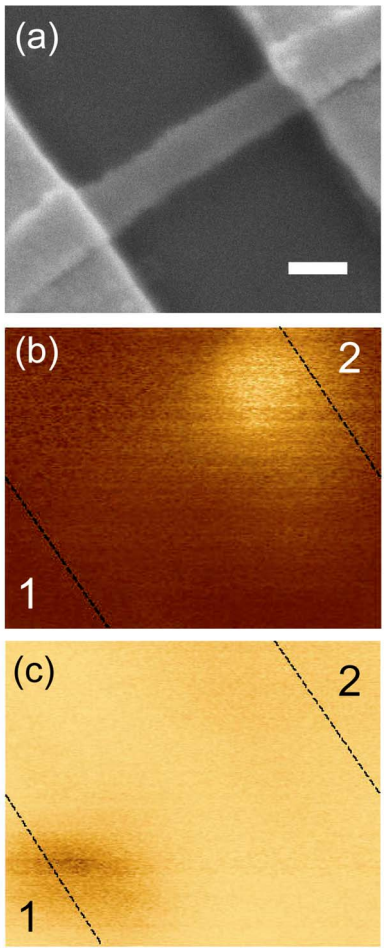

FIG. 2. (Color online) (a) Scanning electron microscopy image of the nanowire photodetector. The scale bar is 200 nm; (b);(c) Photocurrent images for $V_1=2.5$ V (b) and $V_1=-2.5$ V (c). The dashed lines indicate the edges of the electrodes. The scan area is 950×780 nm^2.

~250–300 nm, optical aperture ~50–70 nm, coupled to the laser source) illuminating the area near each of the two contacts, respectively. Unlike the symmetric $I_{ph}-V$ curve seen for global illumination, the local $I_{ph}-V$ curves are asymmetric and produce large photocurrents in only one bias direction. Specifically, the current is largest when the illuminated region corresponds to a reverse-biased M–S diode. This implies that current collection under global illumination may not be occurring uniformly across the entire device.

To elucidate the nature of the NW photoresponse, the local photocurrent was mapped by near-field scanning photocurrent microscopy (NSPM). To realize NSPM, the laser light source was coupled to an NSOM fiber probe, and the photocurrent was recorded as the NSOM probe tip was scanned across the NW photodetector. The resulting photocurrent image provides a two-dimensional map of the photocurrent versus NSOM tip position for a fixed electrode bias. Photocurrent images in which electrode 1 is forward (+2.5 V) and reverse (−2.5 V) biased are shown in Figs. 2(b) and 2(c), respectively. In each case, the photocurrent [represented by the bright and the dark features in Figs. 2(b) and 2(c), respectively] is largest near the reversed-biased contact, that is, near the electrode with the lower bias.

The photocurrent images can be interpreted by considering the NW photodetector as back-to-back Schottky diodes (Fig. 3). When the near-contact region of the reverse (negatively)-biased contact is illuminated [Fig. 3(a)], photogenerated electrons and holes are separated by the strong local electric field, producing the hole current J_{p2} across the M–S interface. In order for the steady-state photocurrent in Fig. 2(b) to be observed, the current continuity condition $|J_{n1}|+|J_{p1}|=|J_{n2}|+|J_{p2}|$ must be met. We propose that the hole current J_{p2} is balanced by the electron current J_{n1} resulting from diffusion of photogenerated electrons across the neutral

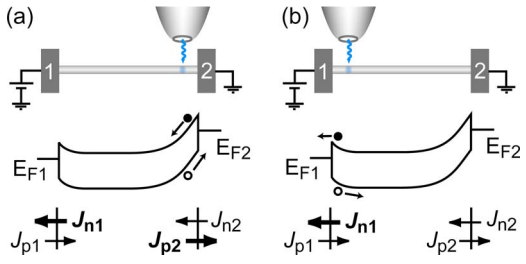

FIG. 3. Schematic diagram of device response to local illumination; (a) illumination of region near reverse-biased M–S contact; (b) illumination of region near forward-biased M–S contact. $J_{n1,2}$ ($J_{p1,2}$) are the electron (hole) currents flowing across the M–S interfaces at electrodes 1 and 2, respectively. Arrows indicate the flow of electrons (solid circles) and holes (circles). The dominant current components are shown in bold type.

region followed by collection at the forward-biased contact 1. We can neglect J_{n2} because of the large barrier at the reverse-biased M–S junction, and J_{p1} can be neglected because it would only become significant under conditions of hole injection, which is not reached at $V_1=2.5$ V as shown in the inset to Fig. 1(a). Because the collection of holes should be efficient in the high electric field near contact 1, we hypothesize that the maximum photocurrent is limited by the diffusion of photogenerated electrons leading to J_{n1}. Under this model, the spatial extent of the photocarrier collection region corresponds to the sum of the hole diffusion length and the width of the space-charge region near the contact.[10]

Within the forward (positively)-biased contact region [Fig. 3(b)], we expect photogenerated electrons to be efficiently collected by contact 1, resulting in J_{n1}. The magnitude of J_{n1} will therefore be determined by the other current components in the continuity equation. The hole current J_{p1} should be negligible since the minority carrier injection from contact 1 is insignificant. Furthermore, we can again neglect J_{n2} because of the large barrier at the M–S junction. We therefore expect $|J_{n1}|\approx|J_{p2}|$, where J_{p2} arises from the photogenerated holes that diffuse across the neutral region and are then collected by contact 2. A very low photocurrent is observed near contact 1 in Fig. 2(b), however; because holes (minority carriers) have lower mobility[11] ($\mu_p \sim 6-48$ cm^2/Vs) than electrons ($\mu_n \sim 300$ cm^2/Vs) in CdS, and minority carriers are expected to have a shorter lifetime than the majority carriers, hole diffusion in Fig. 3(b) may lead to greater carrier losses than for the electron diffusion of Fig. 3(a). Consequently, the strongest photocurrent appears near the reverse-biased electrode in Fig. 2(b). It is important to note that the argument is still valid for a small drift current in the middle of the device. A field would be present in the middle of the device if, for example, the potential drop is not limited to the M–S contact space-charge region. For local illumination in the middle of the NW, the apparent absence of an electric field suggests that photogenerated electrons and holes are not separated, and will recombine with each other rather efficiently. As a result, no photocurrent is observed.

Finally, we note that the saturation observed in both the global and the local $I-V$ curves of Fig. 1 is consistent with the photocurrent being limited by carrier diffusion, since carrier diffusion in a field-free region will not be affected by the bias. For a NW device whose length is comparable to the collection region observed in the NSPM images, one would expect to recover the conventional bulk device behavior because the potential drop would extend across the entire device. Studies of the effect of channel length on device performance are underway. More generally, the NSPM techniques described here can be readily extended to other devices with similar geometries, including transistors, sensors, and light emitting diodes. NSPM therefore has the potential to significantly advance the understanding and development of NW device technology.

This work was supported by Northwestern University, the Semiconductor Research Corporation, the National Science Foundation, and the David and Lucille Packard Foundation. J.L.L. acknowledges the support of a National Science Foundation Graduate Research Fellowship.

[1] J. F. Wang, M. S. Gudiksen, X. F. Duan, Y. Cui, and C. M. Lieber, Science **293**, 1455 (2001).
[2] M. Freitag, Y. Martin, J. A. Misewich, R. Martel, and P. H. Avouris, Nano Lett. **3**, 1067 (2003).
[3] A. Fujiwara, Y. Matsuoka, H. Suematsu, N. Ogawa, K. Miyano, H. Kataura, Y. Maniwa, S. Suzuki, and Y. Achiba, Jpn. J. Appl. Phys., Part 2 **40**, L1129 (2001).
[4] M. Kang, J. S. Lee, S. K. Sim, H. Kim, K. Cho, G. T. Kim, M. Y. Sung, S. Kim, and H. S. Han, Jpn. J. Appl. Phys., Part 1 **43**, 6868 (2004).
[5] K. Balasubramanian, Y. W. Fan, M. Burghard, K. Kern, M. Friedrich, U. Wannek, and A. Mews, Appl. Phys. Lett. **84**, 2400 (2004).
[6] C. J. Barrelet, Y. Wu, D. C. Bell, and C. M. Lieber, J. Am. Chem. Soc. **125**, 11498 (2003).
[7] J. B. D. Soole and H. Schumacher, IEEE J. Quantum Electron. **27**, 737 (1991).
[8] S. M. Sze, *Physics of Semiconductor Devices*, 2nd ed. (Wiley, New York, 1981).
[9] S. E. Ahn, J. S. Lee, H. Kim, S. Kim, B. H. Kang, K. H. Kim, and G. T. Kim, Appl. Phys. Lett. **84**, 5022 (2004).
[10] We observe relatively small changes in the width of the collection region as a function of the bias. One possible explanation is that the hole diffusion length is much greater than the depletion length in the nanowire.
[11] O. Madelung, *Semiconductors-Basic Data* (Springer, Berlin, 1996).